ELSEVIER

Dynamics of Atmospheres and Oceans
34 (2001) 45–71

dynamics of atmospheres and oceans

www.elsevier.com/locate/dynatmoce

The effects of thermal radiation on dry convective instability

Vincent E. Larson*

Program of Atmospheric, Oceans and Climate Bldg. 54, Room 1524 Massachusetts Institute of Technology, P.O. Box 77, Massachusetts Avenue Cambridge, MA 02139-4307, USA

Received 23 November 1998; received in revised form 6 April 2001; accepted 10 April 2001

Abstract

We study the linear and nonlinear stability properties of an idealized radiative–convective model due to Goody. Goody's model is similar to Rayleigh–Bénard convection except that thermal radiative transfer is included, thereby altering the basic state temperature profile and introducing radiative damping. When thermal diffusivity vanishes, we analytically calculate the critical threshold for linear stability. This threshold turns out to have a simple interpretation in terms of a radiative Rayleigh number. This analytic solution has relevance when thermal diffusivity is small but nonzero, because the linear stability threshold for small diffusivity reduces to that for zero thermal diffusivity. The two cases differ, however, in their eigenmodes for temperature perturbations.

When thermal diffusivity is zero, the energy method is used to rule out subcritical instabilities. When thermal diffusivity is nonzero, the energy method is used to find a critical threshold below which all infinitesimal and finite-amplitude perturbations are stable.

Keywords: Radiative–convective model; Rayleigh number; Linear stability; Energy method; Subcritical instability

1. Introduction

Rayleigh–Bénard convection has attracted much attention among fluid dynamicists because it serves as a simple paradigm of fluid mechanical stability and turbulence. Meteorologists, however, have not devoted as much attention to Rayleigh–Bénard convection, primarily because it suffers from several shortcomings as a model of atmospheric convection. The limitation which this paper addresses is that Rayleigh–Bénard convection does not

* Present address: Atmospheric Science Group, Department of Mathematical Sciences, University of Wisconsin-Milwaukee, P.O. Box 413, Milwaukee, WI 53201, USA. Fax: +1-414-229-4907.
E-mail address: vlarson@uwm.edu (V.E. Larson).

0377-0265/01/$ – see front matter
PII: S0377-0265(01)00060-4

include thermal radiative transfer, whereas in a radiative–convective atmosphere, radiation largely determines the basic state and also damps temperature perturbations. For the case of Rayleigh–Bénard convection, many simple linear and nonlinear stability results have been established (see, e.g. Drazin and Reid, 1981; Joseph, 1965). This paper derives some equally simple linear and nonlinear stability properties for an idealized fluid mechanical system in which thermal radiation is added to Rayleigh–Bénard convection. Our goal is to improve physical intuition about the effects of thermal radiative transfer on convection.

In a seminal paper, Goody and Yong (1956a) studied the linear stability of a fluid layer that is confined between parallel plates at specified temperatures, like Rayleigh–Bénard convection, but that is also subject to thermal radiative transfer. The atmosphere has no analog to an upper plate at which temperature is fixed, but Goody's model has some advantages over a more faithful model of the atmosphere. First, theoretical predictions for the model can be tested by laboratory experiments, as demonstrated by Gille and Goody (1964). To the author's knowledge, no further experimental tests of Goody's model have been reported in the literature, although such tests could be made more precise with present technology. Second, results from Goody's model can be compared directly with those from Rayleigh–Bénard convection, thereby isolating the effects of thermal radiative transfer on convective stability. Goody noted that radiation introduces two stabilizing effects on the onset of Rayleigh–Bénard convection. First, radiative damping tends to diminish temperature perturbations. Second, radiation causes the basic state temperature profile in the interior of the domain to have a more stable lapse rate. (In the earth's atmosphere, on the contrary, thermal radiation tends to set up a radiative equilibrium basic state which is convectively unstable.)

Goody (1956a) used a variational technique and a grey, two-stream radiative model to find the critical conditions for linear stability. He considered the limits of optically thin and thick gases, and free-slip, optically black boundaries. Following papers treated more realistic systems and made further calculations. Spiegel (1960) considered the full range of optical depths, proved exchange of stabilities for a linear basic state temperature profile $\bar{T}$, and introduced an approximate stability criterion in the form of a radiative Rayleigh number. Christophorides and Davis (1970) studied the separate contributions of the basic state temperature profile and radiative damping to convective stability, and made calculations of the vertical heat flux when convection ensues. Arpaci and Gozum (1973) considered the effects of nongrey fluids and boundary emissivities. Bdeoui and Soufiani (1997) provide a sophisticated treatment of nongrey fluids and also a short review of prior work. Vincenti and Traugott (1971) also provide a review.

Since our goal is to gain physical intuition, we eschew the trend toward more elaborate models. Instead, we study Goody's model in the limit of a transparent gas. We contribute mainly two new results. First, we simplify Goody's model by setting the thermal diffusivity κ to 0, and obtain a complete analytic solution to the linear stability problem. The linear stability threshold is exactly determined by a single parameter, a radiative Rayleigh number, which resembles the Rayleigh number used to characterize the onset of Rayleigh–Bénard convection. It turns out that when $\kappa \to 0$, we recover several of the $\kappa = 0$ results; hence the intuition associated with the radiative Rayleigh number still has relevance when thermal diffusivity is present. Second, we study the nonlinear stability properties of Goody's model. When $\kappa = 0$, we prove that no subcritical instabilities can

exist, as in Rayleigh–Bénard convection Joseph (1965). When $\kappa \neq 0$, we cannot rule out subcritical instability, but we do find a threshold below which the system is stable to any perturbations, regardless of magnitude; below this threshold, the basic state is monotonically stable.

2. Governing equations

The model that we study consists of a horizontally infinite slab of fluid bounded by upper and lower solid, free-slip boundaries. Although the model is more appropriate to a laboratory flow than a meteorological flow, meteorological applications motivate the choice of parameter values in some of our calculations. A non-zero adiabatic lapse rate $\Gamma_* = g_*/c_{p_*}$ is included in the equations because the lapse rate is significant in the atmosphere (although not in the laboratory). (In this paper, asterisks shall denote dimensional quantities.) Thermal radiation is absorbed but not scattered by the fluid. Solar radiation is neglected. We assume the fluid is radiatively grey — that is, its optical properties are taken to be independent of the wavelength of radiation — even though atmospheric gases are nongrey. This assumption is somewhat unrealistic because it restricts the fluid to one radiative length scale, the photon mean free path. However, the assumption of a grey gas makes analytic progress possible. We consider only transparent fluid layers, that is, fluid layers with small optical depth. This is the appropriate limit for shallow layers in the laboratory.

Following Spiegel and Veronis (1960), we adopt the Boussinesq approximation for an ideal gas, valid when the depth of the system h_* is much less than the scale heights of pressure, density and temperature, and when the motion-induced fluctuations in pressure and density are less than or equal to the corresponding variations in the basic state. In the Boussinesq approximation, the momentum equation is

$$\frac{\partial \boldsymbol{v}_*}{\partial t_*} + \boldsymbol{v}_* \cdot \nabla \boldsymbol{v}_* = -\frac{1}{\rho_*}\nabla_* p'_* + g_* \alpha_{T_*} T'_* \boldsymbol{k} + \nu_* \nabla_*^2 \boldsymbol{v}_*, \tag{1}$$

where $\boldsymbol{v}_*$ is the velocity, T'_* the temperature perturbation from the basic state temperature $\bar{T}_*$, p'_* the pressure perturbation, t_* the time, ρ_* a constant reference density, α_{T_*} the constant volume coefficient of expansion, $\boldsymbol{k}$ the unit vertical vector, ν_* the kinematic viscosity, and g_* the gravitational constant. The momentum equation remains entirely unaltered by radiation. The heat equation becomes

$$\frac{\partial T_*}{\partial t_*} + \boldsymbol{v}_* \cdot \nabla_* T_* + w_* \Gamma_* = -\frac{1}{\rho_* c_{p_*}} \nabla_* \cdot \boldsymbol{F}_* + \kappa_* \nabla_*^2 T_*. \tag{2}$$

Here $T_* = \bar{T}_* + T'_*$ is the total temperature, w_* the vertical component of $\boldsymbol{v}_*$, $\boldsymbol{F}_*$ the flux of radiative energy, c_{p_*} the specific heat at constant pressure, $\Gamma_* = g_*/c_{p_*}$ the adiabatic lapse rate, and κ_* the thermal diffusivity. In the Boussinesq approximation, the continuity equation becomes

$$\nabla_* \cdot \boldsymbol{v}_* = 0. \tag{3}$$

An equation governing the radiative flux $\boldsymbol{F}_*$ can be derived by making the Eddington (two-stream) approximation to Schwartzschild's equation of transfer, as in Goody and Yung (1989) or Goody (1956a). The result is

$$\nabla_* \frac{1}{\alpha_*} \nabla_* \cdot \boldsymbol{F}_* - 3\alpha_* \boldsymbol{F}_* = 4\nabla_* \sigma_* T_*^4, \tag{4}$$

where α_* is the coefficient of absorption of radiation per unit volume, and σ_* the Stefan–Boltzmann constant.

We nondimensionalize these equations with the following scales:

$$\boldsymbol{x}_* = h_* \boldsymbol{x}, \qquad t_* = t_{T_{\mathrm{m}_*}} t, \qquad T_* = \mathcal{T}_* T, \qquad \boldsymbol{v}_* = \frac{h_*}{t_{T_{\mathrm{m}_*}}} \boldsymbol{v},$$

$$p'_* = g_* \alpha_{T_*} \mathcal{T}_* \rho_* h_* p', \qquad \boldsymbol{F}_* = \frac{16}{3} \sigma_* T_{\mathrm{m}_*}^3 \mathcal{T}_* \boldsymbol{F},$$

where

$$t_{T_{\mathrm{m}_*}} \equiv \frac{3}{16} \frac{\rho_* c_{p_*} h_*}{\sigma_* T_{\mathrm{m}_*}^3},$$

and T_{m_*} is the basic state temperature $\bar{T}$ evaluated at the midpoint of the layer. The length scale h_* is the depth of the fluid layer, the time scale $t_{T_{\mathrm{m}_*}}$ is a radiative cooling time scale, and the velocity scale is the velocity of a parcel which travels a distance h_* in a time $t_{T_{\mathrm{m}_*}}$. All temperatures are nondimensionalized with the temperature scale $\mathcal{T}_*$, which can be freely specified as convenient. Unless otherwise noted, this paper shall set $\mathcal{T}_* = T_{\mathrm{L}_*} - T_{\mathrm{U}_*}$, where T_{L_*} is the temperature of the lower plate and T_{U_*} the temperature of the upper plate. The nondimensionalized momentum, heat, continuity, and radiative transfer equations are, respectively,

$$\chi \frac{\partial \boldsymbol{v}}{\partial t} + \chi \boldsymbol{v} \cdot \nabla \boldsymbol{v} = -\gamma \nabla p' + \gamma T' \boldsymbol{k} + \nabla^2 \boldsymbol{v}, \tag{5}$$

$$\frac{\partial T}{\partial t} + \boldsymbol{v} \cdot \nabla T + w\Gamma = -\nabla \cdot \boldsymbol{F} + \kappa \nabla^2 T, \tag{6}$$

$$\nabla \cdot \boldsymbol{v} = 0, \tag{7}$$

and

$$\nabla \frac{1}{\alpha} \nabla \cdot \boldsymbol{F} - 3\alpha \boldsymbol{F} = 3\nabla T, \tag{8}$$

where we have linearized the thermal source function on the right-hand side of the radiation equation (8). The specified dimensionless constants and function that govern the behavior of the system are defined as follows:

$$\gamma = \frac{g_* \alpha_{T_*} \mathcal{T}_* h_*^3}{\nu_* (h_*^2 / t_{T_{\mathrm{m}_*}})}, \qquad \kappa = \frac{\kappa_*}{h_*^2 / t_{T_{\mathrm{m}_*}}}, \qquad \Gamma = \frac{\Gamma_*}{\mathcal{T}_* / h_*} = \frac{g_* / c_{p_*}}{\mathcal{T}_* / h_*},$$

$$\alpha(z) = \alpha_*(z_*) h_*, \qquad \chi = \frac{16 \sigma_* T_{\mathrm{m}_*}^3 h_*}{3 \rho_* c_{p_*} \nu_*} = \frac{h_*^2 / t_{T_{\mathrm{m}_*}}}{\nu_*}.$$

Here γ is a coefficient, akin to a Rayleigh number, which multiplies the buoyancy term in the momentum equation. κ is a nondimensional thermal diffusivity which measures the strength of thermal diffusivity relative to a "radiative diffusivity" $h_*^2/t_{T_{m_*}}$. For a typical dry atmospheric boundary layer of depth $h_* = 1\,\mathrm{km}$ and $T_{m_*} = 285\,\mathrm{K}$, $\kappa \sim 3 \times 10^{-6}$; an appropriate value for a laboratory-sized system is $\kappa \sim 0.1$. Therefore, this paper selects values of κ which range from very low values to moderate values. Γ is a dimensionless adiabatic lapse rate. α_c is simply the optical depth of the layer in the case that $\alpha = \alpha_c$ is constant. Otherwise, $\alpha(z)$ represents the number of photon mean free paths per layer depth, at the local value of $\alpha_*(z_*)$. The quantity χ is an inverse radiative Prandtl number which turns out not to enter our stability thresholds, since it only multiplies time-dependent and nonlinear terms.

We choose solid, free-slip, constant-temperature boundaries located at $z = \pm 1/2$. This leads to the boundary conditions (Drazin and Reid, 1981)

$$w|_{z=\pm 1/2} = \left.\frac{\partial^2 w}{\partial z^2}\right|_{z=\pm 1/2} = 0.$$

When $\kappa \neq 0$,

$$T'|_{z=\pm 1/2} = 0.$$

3. Linear stability equations

In this section, we write down the linear stability equations.

We postulate a basic state in which $\boldsymbol{v} = 0$, and in which the temperature $\bar{T} = \bar{T}(z)$, radiative flux $\bar{\boldsymbol{F}} = \bar{F}_z(z)\boldsymbol{k}$, and radiative absorption coefficient $\alpha = \alpha(z)$ are functions of z alone. Substituting these forms into the heat equation (6) and the radiative transfer equation (8) leads to, respectively,

$$0 = -\frac{\mathrm{d}\bar{F}_z}{\mathrm{d}z} + \kappa \frac{\mathrm{d}^2\bar{T}}{\mathrm{d}z^2} \tag{9}$$

and

$$\frac{\mathrm{d}}{\mathrm{d}z}\frac{1}{\alpha}\frac{\mathrm{d}\bar{F}_z}{\mathrm{d}z} - 3\alpha\bar{F}_z = 3\frac{\mathrm{d}\bar{T}}{\mathrm{d}z}. \tag{10}$$

We now obtain perturbation equations about the basic state. Subtracting the basic state radiative equation (10) from the full radiative equation (8), we obtain an equation for the perturbation radiative flux $\boldsymbol{F}'$

$$\nabla\frac{1}{\alpha}\nabla\cdot\boldsymbol{F}' - 3\alpha\boldsymbol{F}' = 3\nabla T'. \tag{11}$$

(We have neglected perturbations in α.) For transparent fluid layers — more specifically, those with $\alpha^2 \ll a^2$, where a is the wavenumber of the unstable mode under consideration — we may neglect the $3\alpha\boldsymbol{F}'$ term. Consequently,

$$\nabla\cdot\boldsymbol{F}' \cong 3\alpha T'. \tag{12}$$

The integration constant has been set to 0 because a zero-temperature perturbation requires that there be no perturbative contribution to the radiative cooling. equation (12) is the Newtonian approximation (Goody, 1995). This limit is of interest to meteorologists because, although our derivation is for a transparent grey gas, the Newtonian approximation is also a common meteorological approximation for nongrey, noncloudy atmospheres. In these cases, the perturbation radiative heating is dominated by the cooling-to-space contribution, and the divergence of the perturbation radiative flux is again proportional to T', as shown by Goody (1995). We obtain a perturbation temperature equation upon subtracting the basic state heat equation (9) from the full heat equation (6), using the Newtonian approximation (12), and linearizing

$$\frac{\partial T'}{\partial t} + w\left(\frac{\mathrm{d}\bar{T}}{\mathrm{d}z} + \Gamma\right) = -3\alpha T' + \kappa\nabla^2 T'. \tag{13}$$

Applying the operator $\boldsymbol{k}\cdot\nabla\times\nabla$ to the momentum equation (5), using continuity, and linearizing yields

$$\chi\frac{\partial}{\partial t}\nabla^2 w = \gamma\nabla_{\mathrm{h}}^2 T' + \nabla^2\nabla^2 w, \tag{14}$$

where

$$\nabla_{\mathrm{h}}^2 \equiv \frac{\partial^2}{\partial x^2} + \frac{\partial^2}{\partial y^2}$$

is the horizontal Laplacian. We have used the continuity equation (7) here. Eliminating T' from equation (14) and the linearized heat equation (13) leaves an equation for w alone

$$\left(\frac{\partial}{\partial t} + 3\alpha - \kappa\nabla^2\right)\left(\chi\frac{\partial}{\partial t} - \nabla^2\right)\nabla^2 w = -\left(\frac{\mathrm{d}\bar{T}}{\mathrm{d}z} + \Gamma\right)\gamma\nabla_{\mathrm{h}}^2 w. \tag{15}$$

We seek normal mode solutions of the form

$$w = Re\{W(z)f(x,y)\,\mathrm{e}^{st}\}, \qquad T' = Re\{\Theta'(z)f(x,y)\,\mathrm{e}^{st}\} \tag{16}$$

where

$$\nabla_{\mathrm{h}}^2 f(x,y) = -a^2 f(x,y),$$

and a is a real, nondimensionalized horizontal wavenumber. The planform of convection, which is described by $f(x,y)$, is left undetermined by linear stability analysis. In general, s can be complex: $s = \sigma + \mathrm{i}\omega$, where the growth rate σ is a real constant and so is ω. Substituting the modal forms equation (16) into the linear equations for w (14) and T' (13) yields, respectively,

$$\chi s(D^2 - a^2)W = -\gamma a^2\Theta' + (D^2 - a^2)^2 W \tag{17}$$

and

$$s\Theta' = -W\left(\frac{\mathrm{d}\bar{T}}{\mathrm{d}z} + \Gamma\right) - 3\alpha\Theta' + \kappa(D^2 - a^2)\Theta', \tag{18}$$

where the operator $D \equiv \mathrm{d}/\mathrm{d}z$. Likewise, substituting the modal form equation (16) for w into the linear stability equation (15) yields

$$[s + 3\alpha - \kappa(D^2 - a^2)][\chi s - (D^2 - a^2)](D^2 - a^2)W(z) = \left(\frac{\mathrm{d}\bar{T}}{\mathrm{d}z} + \Gamma\right)\gamma a^2 W(z). \tag{19}$$

Mathematically, radiation enters the equation through the radiative damping term 3α and the basic state temperature gradient $\mathrm{d}\bar{T}/\mathrm{d}z$.

Exchange of stabilities holds if it is true that whenever the growth rate $\sigma = 0$, also $\omega = 0$. Then, s passes from negative growth rate to positive growth rate through the origin ($\omega = 0$). In this case, convection arises as overturning cells whose amplitude increases monotonically in time. Alternatively, if $\omega \neq 0$ as σ approaches 0, then oscillatory instability or overstability sets, (Drazin and Reid, 1981). When exchange of stabilities holds, one may set $s = 0$ in a linear stability analysis, thereby facilitating theory and numerical calculations.

Exchange of stabilities does hold for the case of interest to us, namely constant $\alpha \equiv \alpha_c$ and free-slip constant-temperature boundary conditions. This can be seen by inspecting the derivation of Murgai and Khosla (1962). They studied exchange of stabilities for a system that includes a vertical magnetic field. Exchange of stabilities for our problem follows if the magnetic field in their analysis is set to 0. One difficulty in proving exchange of stabilities is the fact that when radiation is introduced into the convection problem, the basic state temperature profile $\bar{T}(z)$ is no longer linear. A key to Murgai and Khosla's proof is to eliminate Θ'. Then, $\mathrm{d}\bar{T}/\mathrm{d}z$ turns out to appear as a prefactor of a term with no imaginary part. Hence, $\mathrm{d}\bar{T}/\mathrm{d}z$ drops out of the evaluation of the imaginary part of the growth rate. Spiegel (1962) and Veronis (1963) also illustrated this technique. In a similar manner, one can prove exchange of stabilities when $\kappa = 0$, for free-slip and no-slip boundaries. When $\kappa = 0$, the boundary conditions on temperature are dropped.

4. Linear stability with no thermal diffusivity

In this section, we explore a minimal radiative–convective model. We let $\alpha \equiv \alpha_c$ be a constant and neglect the thermal diffusivity of heat entirely by setting $\kappa = 0$. All damping of temperature perturbations is then due to radiation. These simplifying approximations permit a complete analytic solution for the linear stability problem. A similar analysis for an idealized atmospheric radiative–convective model has been performed by Larson (2000).

In the atmosphere, thermal diffusive damping is much smaller than radiative damping. Section 5 shows that when κ is small but non-vanishing, the critical condition for linear stability approaches that for the $\kappa = 0$ case. Therefore, the $\kappa = 0$ results constitute an important limiting case.

First, we find the basic state for the linear stability analysis. The basic state heat equation (9) implies that

$$\bar{F}_z = F_T,$$

where F_T is a constant which must be determined by the boundary conditions on $\bar{F}_z$. Inserting this relation into the basic state radiation equation (10) yields the basic state temperature gradient

$$\frac{\mathrm{d}\bar{T}}{\mathrm{d}z} = -\alpha_\mathrm{c} F_T \equiv -(T_\mathrm{l} - T_\mathrm{u}), \tag{20}$$

where T_l and T_u denote the (nondimensionalized) temperatures of the fluid adjacent to the lower and upper boundaries, respectively. The temperature decreases linearly with altitude. Such a simple profile would not have resulted if we had not linearized the radiative equation (8), which is valid if the temperature difference across the depth of the layer is small.

We formulate radiative boundary conditions following the procedure in Goody (1995, pp. 114–115). Assuming that the temperature difference across the layer is small and that the Eddington approximation holds, we obtain, for the upper and lower boundaries, respectively,

$$T_\mathrm{U} - T_\mathrm{u} = -\tfrac{2}{3}\bar{F}_z|_{z=1/2} = -\frac{2}{3}F_T \tag{21}$$

and

$$T_\mathrm{L} - T_\mathrm{l} = \tfrac{2}{3}\bar{F}_z|_{z=-1/2} = \frac{2}{3}F_T. \tag{22}$$

We have specified the (nondimensionalized) temperatures of the upper and lower boundaries to be T_U and T_L, respectively. There are discontinuities in temperature at the boundaries.

We may now solve for F_T and $\mathrm{d}\bar{T}/\mathrm{d}z$ using Eqs. (20)–(22). F_T is given by

$$F_T = \frac{3/4}{1 + (3/4)\alpha_\mathrm{c}}. \tag{23}$$

Substituting F_T into expression (20) for $\mathrm{d}\bar{T}/\mathrm{d}z$, we find

$$\frac{\mathrm{d}\bar{T}}{\mathrm{d}z} = -\frac{(3/4)\alpha_\mathrm{c}}{1 + (3/4)\alpha_\mathrm{c}}. \tag{24}$$

(Recall that $T_\mathrm{L} - T_\mathrm{U} \equiv 1$.) The smaller the optical depth, the smaller the magnitude of $\mathrm{d}\bar{T}/\mathrm{d}z$. Hence, smaller optical depths imply more stable basic states.

We now find the marginally stable modes when $\alpha = \alpha_\mathrm{c}$ is constant and the thermal diffusivity is neglected. Since exchange of stabilities holds, $s = 0$ at the onset of instability. Also recall that we are assuming $\kappa = 0$. Hence, the stability equation (19) for W becomes

$$3\alpha_\mathrm{c}(D^2 - a^2)^2 W(z) = -\left(\frac{\mathrm{d}\bar{T}}{\mathrm{d}z} + \Gamma\right)\gamma a^2 W(z). \tag{25}$$

As in Rayleigh–Bénard convection, the eigenfunctions are sinusoidal. The gravest mode is

$$W(z) = \cos \pi z, \tag{26}$$

$$\Theta'(z) = \frac{(\pi^2 + a^2)^2}{\gamma a^2} \cos \pi z. \tag{27}$$

Substituting this form for $W(z)$ into the stability equation (25) yields a critical condition on $\gamma = \gamma_{\mathrm{m}}$ for marginal stability,

$$-\left(\frac{\mathrm{d}\bar{T}}{\mathrm{d}z} + \Gamma\right)\frac{\gamma_{\mathrm{m}}}{3\alpha_{\mathrm{c}}} = \frac{(\pi^2 + a^2)^2}{a^2}.$$

Whereas the classical Rayleigh–Bénard system first goes unstable at $a = \pi/\sqrt{2}$ (Drazin and Reid, 1981), our system does so at a shorter wavelength corresponding to $a = \pi$. Therefore, the critical value of $\gamma = \gamma_{\mathrm{C}}$ is

$$-\left(\frac{\mathrm{d}\bar{T}}{\mathrm{d}z} + \Gamma\right)\frac{\gamma_{\mathrm{C}}}{3\alpha_{\mathrm{c}}} = 4\pi^2. \tag{28}$$

In the critical condition, all the individual governing parameters — $\gamma_{\mathrm{C}}, \alpha_{\mathrm{c}}$, and $-((\mathrm{d}\bar{T}/\mathrm{d}z) + \Gamma)$ — are conveniently lumped together into one factor on the left-hand side. This factor can be interpreted as a radiative Rayleigh number

$$Ra_{\mathrm{R}} = -\left(\frac{\mathrm{d}\bar{T}}{\mathrm{d}z} + \Gamma\right)\frac{\gamma}{3\alpha_{\mathrm{c}}}$$

with critical value $Ra_{\mathrm{RC}} = 4\pi^2$. If we define a "radiative diffusivity" [1]

$$\kappa_{\mathrm{R}_*} \equiv \frac{16\sigma_* T_{\mathrm{m}_*}^3 \alpha_{\mathrm{c}_*} h_*^2}{\rho_* c_{p_*}} = \nu_* 3\alpha_{\mathrm{c}}\chi$$

and a lapse rate difference from adiabatic

$$\beta_* = \frac{(3/4)\alpha_{\mathrm{c}_*} h_*}{1 + (3/4)\alpha_{\mathrm{c}_*} h_*}\frac{(T_{\mathrm{L}_*} - T_{\mathrm{U}_*})}{h_*} - \frac{g_*}{c_{p_*}},$$

then the radiative Rayleigh number becomes

$$Ra_{\mathrm{R}} = \frac{g_*\alpha_{T_*}\beta_* h_*^4}{\nu_*\kappa_{\mathrm{R}_*}} = \frac{g_*\alpha_{T_*}\left(\frac{\frac{3}{4}\alpha_{\mathrm{c}_*} h_*}{1+(\frac{3}{4})\alpha_{\mathrm{c}_*} h_*}\frac{(T_{\mathrm{L}_*} - T_{\mathrm{U}_*})}{h_*} - \frac{g_*}{c_{p_*}}\right) h_*^4}{\nu_*\frac{16\sigma_* T_{\mathrm{m}_*}^3 \alpha_{\mathrm{c}_*} h_*^2}{\rho_* c_{p_*}}}. \tag{29}$$

Despite the complexity introduced by radiation, the critical condition depends on only one parameter, as in Rayleigh–Bénard convection. This parameter, Ra_{R}, is like the standard Rayleigh number, except that β_* is the *interior* temperature gradient (which does not include the temperature jumps at the boundaries) and κ_{R_*} is a radiative diffusivity, not the thermal diffusivity. Spiegel and Veronis (1960) used an approximate variational technique and physical arguments to derive and interpret a similar radiative Rayleigh number. Goody (1964) also discusses a similar radiative Rayleigh number.

[1] The terminology "radiative diffusivity" has been introduced to highlight the analogous role of radiation and molecular diffusion in transporting heat in the Goody and Rayleigh–Bénard models. The radiative diffusivity can be thought of merely as a length scale squared divided by a radiative time scale. We do not mean to imply that radiative transfer in a transparent medium is a local, diffusive-like process.

One can assess the effect of any dimensional parameter on the linear stability threshold by inspecting Ra_{R}. For instance, an increase in T_{m_*} leads to a stabilizing increase in the radiative diffusivity κ_{R_*} but has no effect on the lapse rate parameter β_*, because we have specified the temperature on the boundaries. Furthermore, the specific dependence is seen to be $Ra_{\mathrm{R}} \propto T_{\mathrm{m}_*}^{-3}$. Also, increasing α_{c_*} leads to a stabilizing linear increase in κ_{R_*} but also leads to a more unstable β_*. The net effect depends on the lapse rate g_*/c_{p_*}.

5. Linear stability with thermal diffusivity

When $\kappa = 0$, a temperature profile may be stable even though there are temperature discontinuities in the unstable sense at the boundaries. The temperature discontinuities do not lead to instability because there exists no thermal diffusivity to communicate heat from the boundaries to the adjacent fluid. When a small amount of thermal diffusivity is added, however, one might suppose that the solutions change fundamentally. After all, $\kappa = 0$ multiplies the highest derivative in the heat equation (6). Therefore, $\kappa \to 0$ is a singular limit. It turns out, however, that in many cases the addition of a small but nonzero thermal diffusivity term does not qualitatively alter either the threshold for marginal stability γ_{m} or the vertical velocity linear modes. But the qualitative aspects of the solution are not left entirely unchanged. Rather, the temperature perturbation linear modes Θ' develop thin boundary layers. To show this, we now permit non-zero values of κ. We also set $\alpha = \alpha_{\mathrm{c}} =$ constant. This is the problem first studied in the seminal paper by Goody (1956a).

Goody (1956a) derived boundary conditions on radiation using the assumption that thermal diffusivity causes temperatures infinitesimally close to the boundaries to equal the temperatures of the boundaries themselves. The conditions are

$$\left.\frac{\mathrm{d}\bar{F}_z}{\mathrm{d}z}\right|_{z=1/2} = -2\alpha_{\mathrm{c}}\bar{F}_z|_{z=1/2}, \qquad \left.\frac{\mathrm{d}\bar{F}_z}{\mathrm{d}z}\right|_{z=-1/2} = 2\alpha_{\mathrm{c}}\bar{F}_z|_{z=-1/2}. \tag{30}$$

With these conditions, Goody (1956a) derived the following basic state temperature profile:

$$\frac{\mathrm{d}\bar{T}}{\mathrm{d}z} = -L\cosh\lambda z - M \tag{31}$$

$$\bar{F}_z = \kappa\left(-L\cosh\lambda z + \frac{1}{\kappa\alpha_{\mathrm{c}}}M\right)$$

where

$$L \equiv \frac{1}{\kappa\alpha_{\mathrm{c}}}\left[\frac{2}{\kappa\alpha_{\mathrm{c}}\lambda}\sinh\frac{\lambda}{2} + \frac{1}{2}\frac{\lambda}{\alpha_{\mathrm{c}}}\sinh\frac{\lambda}{2} + \cosh\frac{\lambda}{2}\right]^{-1},$$

$$M \equiv L\kappa\alpha_{\mathrm{c}}\left(\frac{1}{2}\frac{\lambda}{\alpha_{\mathrm{c}}}\sinh\frac{\lambda}{2} + \cosh\frac{\lambda}{2}\right) = 1 - \frac{2L}{\lambda}\sinh\frac{\lambda}{2},$$

and

$$\lambda^2 \equiv 3\alpha_{\mathrm{c}}^2\left(1 + \frac{1}{\kappa\alpha_{\mathrm{c}}}\right).$$

Fig. 1 shows sample basic state temperature profiles for $\kappa \neq 0$, along with one profile for

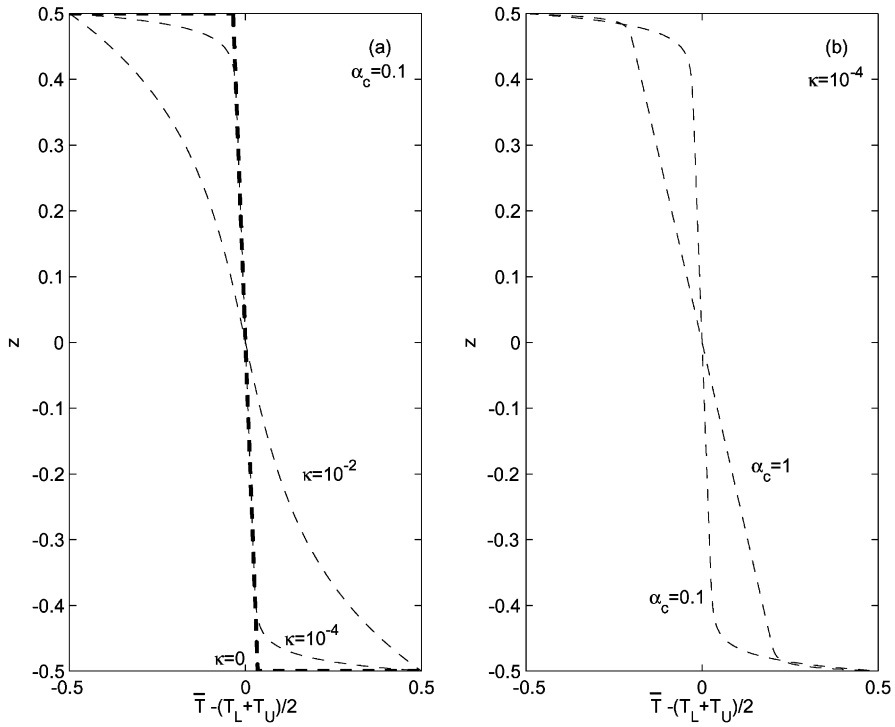

Fig. 1. Shifted basic state temperature profiles $\bar{T} - (T_\mathrm{L} + T_\mathrm{U})/2$ vs. z, for $\kappa \neq 0$ (thin dashed lines) as obtained from equation (31), and for $\kappa = 0$ (thick dashed lines) as obtained from equation (24). In (a), we fix $\alpha_\mathrm{c} = 0.1$ and let $\kappa = 10^{-2}, 10^{-4}, 0$. As the thermal diffusivity κ approaches 0, temperature discontinuities form at the boundaries, and a linear temperature profile forms in the interior. In (b), we fix $\kappa = 10^{-4}$ and let $\alpha_\mathrm{c} = 0.1, 1$. As the optical depth α_c decreases, the interior temperature gradient decreases.

$\kappa = 0$ (thick dashed line). When $\kappa \to 0$, the shape of $\bar{T}$ approaches that for the $\kappa = 0$ case, in which the boundary layers have zero thickness, i.e. are discontinuities. More specifically, when thermal diffusion of features of scale h_* is much weaker than radiative damping (i.e. $\kappa/3\alpha_\mathrm{c} \ll 1$), and the layer is transparent (i.e. $\alpha_\mathrm{c} \leq 1$), the fraction of the layer occupied by the boundary layers goes as $\sqrt{\kappa/3\alpha_\mathrm{c}}$. Furthermore, when $\kappa \to 0$, the value of $\mathrm{d}\bar{T}/\mathrm{d}z$ in the middle of the convecting region tends toward the interior value of $\mathrm{d}\bar{T}/\mathrm{d}z$ when $\kappa = 0$. As α_c decreases, radiation tends to stabilize the profile in the interior more strongly, leaving strongly superadiabatic gradients near the boundaries. In the opposite limit, when thermal diffusivity dominates radiative damping, $\bar{T}$ reduces to the linear profile of Rayleigh–Bénard convection.

We now compute the linear eigenmodes and the marginal Rayleigh number $Ra_\mathrm{m} = \gamma_\mathrm{m}/\kappa$. Because of exchange of stabilities, we may set $s = 0$ in the linear stability equation for W (19)

$$\left((D^2 - a^2) - \frac{3\alpha_\mathrm{c}}{\kappa}\right)(D^2 - a^2)^2 W(z) = Ra\left(\frac{\mathrm{d}\bar{T}}{\mathrm{d}z} + \Gamma\right)a^2\, W(z). \tag{32}$$

Given values of α_c, κ, and a^2, we compute all eigenmodes $W(z)$ and eigenvalues Ra_m numerically and select the least eigenvalue. Details of the numerical method can be found in Appendix A. Numerical computations yield the shape of the eigenmodes explicitly. This is an advantage over the variational method used in most past studies, in which the eigenvalues are computed using a guess or series expansion for the eigenmodes. Similar numerical calculations have also been performed by Getling (1980), but he did not examine the Θ' profiles.

The eigenvalues Ra_m are plotted versus a^2 in Fig. 2. In all our numerical work, we have set $\Gamma = 0$. When κ is small, then the minimum of $Ra_m(a^2)$ usually occurs near the wavenumber $a^2 = \pi^2$, as for the $\kappa = 0$ case. When κ is larger, the curve $Ra_m(a^2)$ reduces to that for Rayleigh–Bénard convection, with a minimum Ra_C at $a^2 = \pi^2/2$.

Some curves contain a kink at higher wavenumbers. This kink is associated with a change in the vertical structure of the eigenmodes. Goody (1956a) hypothesized that the eigenmodes in w might take one of two shapes: a sinusoidal shape which penetrates the full layer depth, as in Rayleigh–Bénard convection; or a shape which is concentrated near the boundaries, where the temperature gradients are strongly superadiabatic. Getling (1980) showed that both types of modes can be realized. Our calculations agree. In Fig. 2, all points with small wavenumbers ($a^2 \leq \pi^2$) correspond to approximately sinusoidal w. At some wavenumber $a^2 \geq \pi^2$, often near a kink in the marginal stability curve, a transition region of about an order of magnitude or two in a^2 exists. By the time $a^2 = 10^5$ has been reached, w exhibits boundary layers for all cases. Long wavelength modes prefer to traverse the full layer from bottom to top. On the contrary, the short-wavelength modes prefer to form two separate overturning layers near the boundaries, rather than form tall, skinny cells that penetrate the full layer. When the modes confine themselves near the boundaries, they can enjoy the superadiabatic temperature gradient there. Thus, for certain parameter values, e.g. $\alpha_c = 0.002$ and $\kappa = 5 \times 10^{-8}$, $\mathrm{d}\bar{T}/\mathrm{d}z$ is small in the interior and large near the boundaries, and the boundary-layer motions become unstable much sooner than the sinusoidal motions (not shown). The change in form of the most unstable mode was suggested by Goody (1956a) and explicitly calculated by Getling (1980).

We now use approximations to (1) understand why boundary layers in $\Theta'(z)$ arise; (2) find a simple estimate of Ra_m; and (3) show that Ra_m for $\kappa \to 0$ approaches Ra_m for $\kappa = 0$, despite the boundary layers in $\Theta'(z)$.

First, we find a simple approximate formula for $\Theta'(z)$. When $a^2 \cong \pi^2$ and $\kappa = 0$, both $W(z)$ and $\Theta'(z)$ are sinusoidal. However, when $a^2 \cong \pi^2$ and $\kappa \to 0$, $W(z)$ still approaches a sinusoid, but $\Theta'(z)$ develops thin boundary layers (although the interior of $\Theta'(z)$ remains nearly sinusoidal). To approximate Θ', we invert the linear stability equation (18) for Θ', assuming that W has the sinusoidal form (26), and that $s = 0$. Then, we find

$$\Theta' \cong \frac{1}{\kappa}\left\{\frac{M-\Gamma}{\pi^2+q^2}\cos\pi z + \frac{L}{(-\pi^2-q^2+\lambda^2)^2+(2\pi\lambda)^2} \times\left(2\pi\lambda\frac{\sinh(1/2)\lambda}{\cosh(1/2)q}\cosh qz - 2\pi\lambda\sin\pi z\sinh\lambda z - (-\pi^2-q^2+\lambda^2)\cos\pi z\cosh\lambda z\right)\right\}, \tag{33}$$

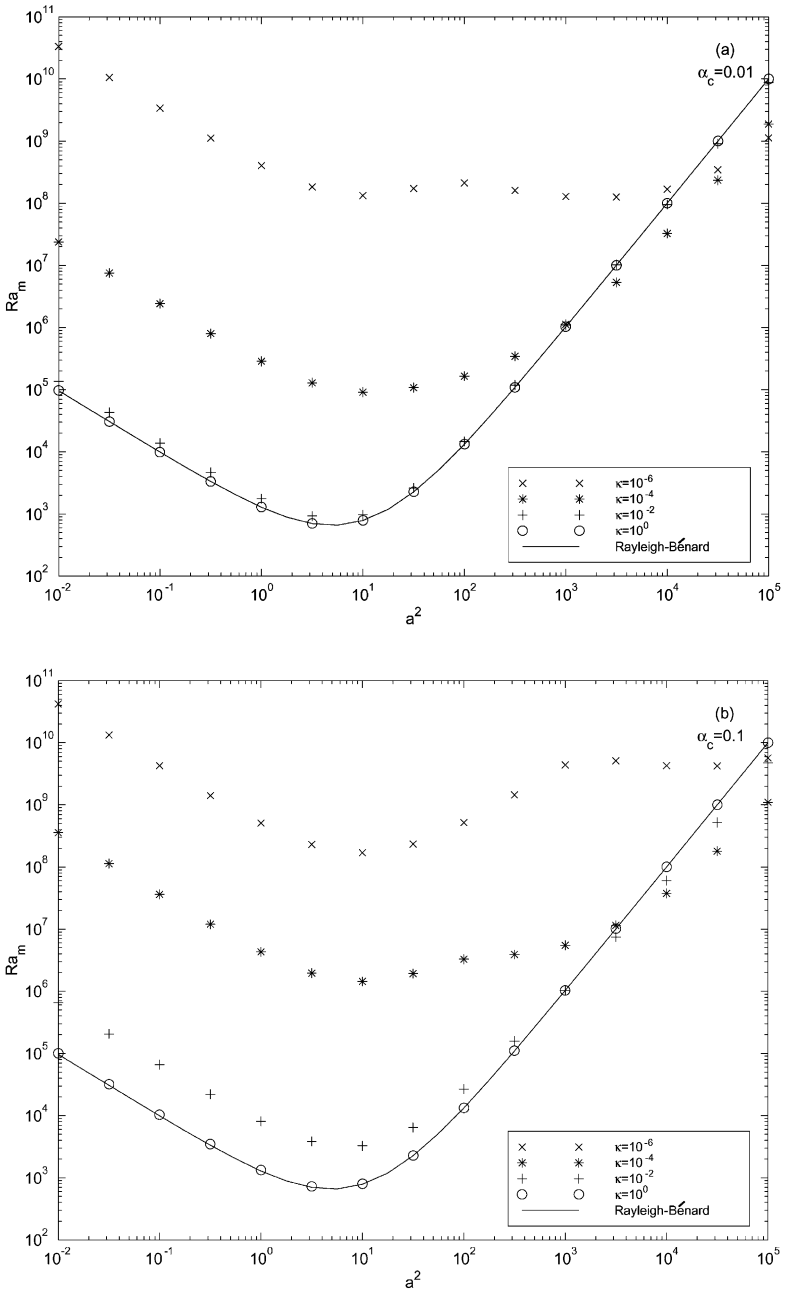

Fig. 2. The Rayleigh number for marginal stability Ra_{m} versus wavenumber squared a^2 obtained from numerical solution of (32). The markers denote the value of κ given in the legends. In parts (a), (b) and (c), the solid line denotes the marginal stability curve for Rayleigh–Bénard convection (which has no radiation). Also in parts (a), (b) and (c), we set $\Gamma = 0$. In (a), $\alpha_{\mathrm{c}} = 0.01$; in (b), $\alpha_{\mathrm{c}} = 0.1$; and in (c), $\alpha_{\mathrm{c}} = 1$. When κ decreases, the basic state temperature profile is stabilized in the interior.

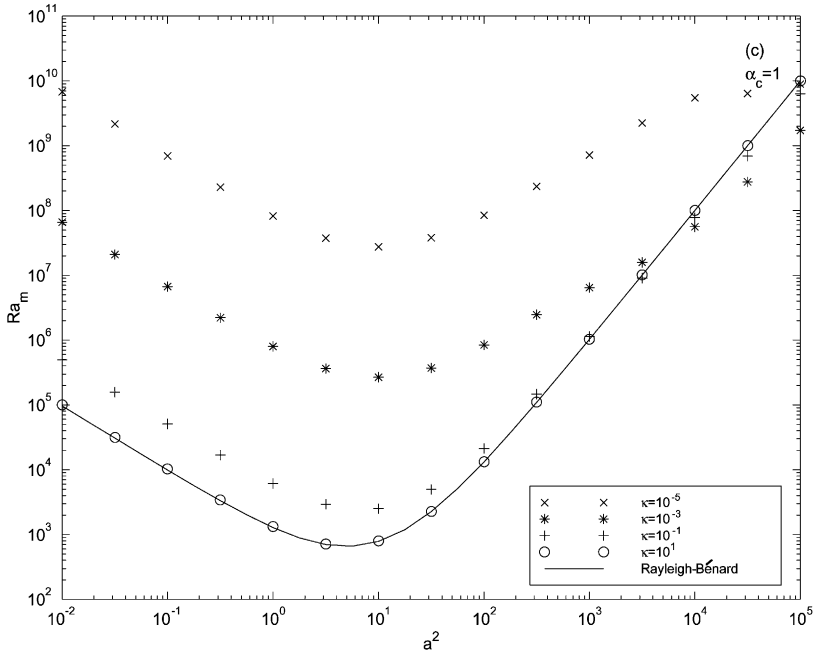

Fig. 2. (*Continued*).

where $q^2 \equiv a^2 + 3\alpha_c/\kappa$. This formula is accurate whenever W is nearly sinusoidal, regardless of the value of κ. The first term on the right-hand side of equation (33) gives rise to the sinusoidal interior of Θ'. As $\kappa \to 0$, the first term reduces exactly to the $\kappa = 0$ eigenmode (27) for Θ' if, in equation (27), we set $a^2 = \pi^2$ and use formula (35) for γ_C below. The remaining terms in the expression (33) for Θ' produce the boundary layers. From this expression, we may deduce that the boundary layers in Θ' occupy a fraction $\sim 1/\lambda$ of the total depth of the layer; this is also true of the boundary layers in $\bar{T}$. It is lifting of fluid parcels in these superadiabatic regions of $\bar{T}$ that gives rise to the boundary layers in Θ'. These features are illustrated in Fig. 3.

We now write down an approximate expression for Ra_m, following Goody (1956a,b). Then, we demonstrate that in the limit $\kappa \to 0$, this expression can be reduced to the critical condition (28) for the $\kappa = 0$ case. In those cases in which we have established numerically that the most unstable mode has a nearly sinusoidal profile for $W(z)$, we can have confidence that the variational method with a sinusoidal trial function for $W(z)$ will yield accurate values of Ra_m. Therefore, we can write

$$Ra_m \cong \frac{\int_{-1/2}^{1/2} dz\, W\{-(D^2 - a^2 - 3\alpha_c/\kappa)(D^2 - a^2)^2 W\}}{a^2 \int_{-1/2}^{1/2} dz(-(d\bar{T}/dz) - \Gamma) W^2}.$$

Substituting into this expression our trial function $W(z) = \cos \pi z$, we find

$$Ra_m = \frac{\gamma_m}{\kappa} \cong \frac{((\pi^2 + a^2)^2/a^2)((\pi^2 + a^2) + 3\alpha_c/\kappa)}{2(2\pi)^2 L((\sinh(1/2)\lambda)/\lambda)(1/(\lambda^2 + (2\pi)^2)) + M - \Gamma}. \tag{34}$$

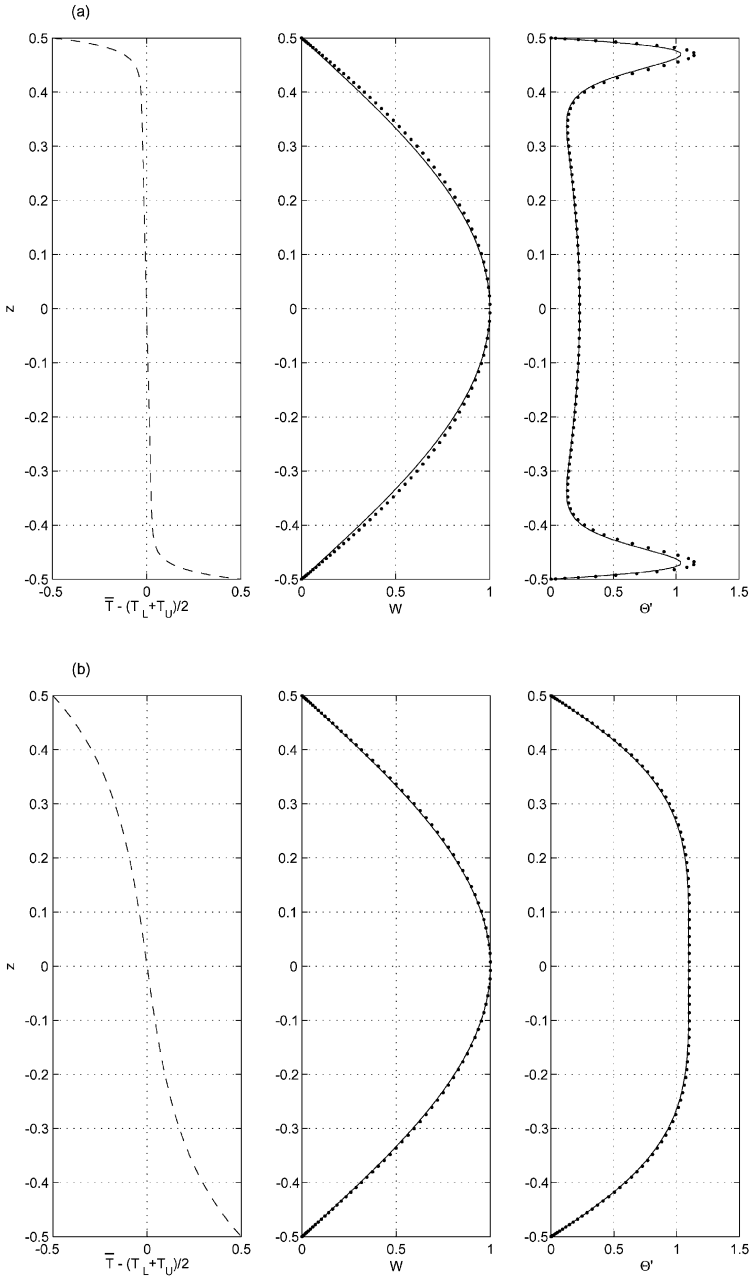

Fig. 3. Linear eigenmodes computed numerically from equation (32) (dots), the approximations to these eigenmodes given by Eqs. (26) and (33) (solid lines), and shifted basic state temperature profiles $\bar{T} - (T_\mathrm{L} + T_\mathrm{U})/2$ (dashed lines). We set $\alpha_\mathrm{c} = 0.1$ and $\Gamma = 0$, and choose the value of a^2 which minimizes γ_m. In (a), $\kappa = 10^{-4}$ and $a^2 = 10.02$; in (b), $\kappa = 10^{-2}$ and $a^2 = 7.260$; and in (c), $\kappa = 1$ and $a^2 = 4.984$. The approximate eigenmodes are adequate over a wide range of κ, if $a^2 \sim \mathcal{O}(\pi^2)$.

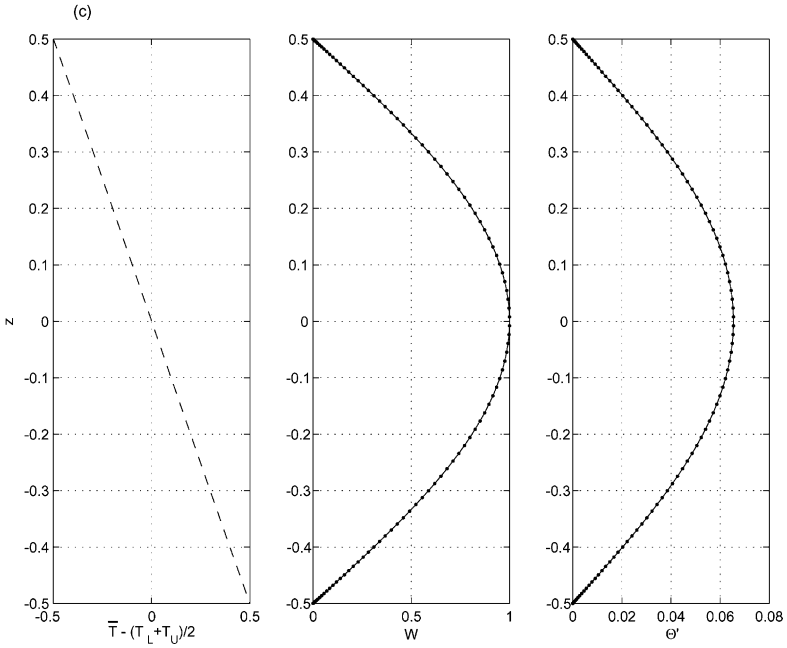

Fig. 3. (*Continued*).

We can approximate γ_m for the case in which κ is small enough. By "small enough", we mean that $3\alpha_c/\kappa \gg (2\pi)^2$ and that

$$\frac{(3/4)\alpha_c}{1+(3/4)\alpha_c} - \Gamma \gg \frac{4\pi^2\kappa}{3\alpha_c}\frac{1}{1+(3/4)\alpha_c}.$$

With small κ, the assumption of optical transparency ($\alpha_c \leq 1$), and the assumption that the most unstable mode has wavenumber $a^2 \cong \pi^2$, the expression (34) becomes

$$\left(\frac{(3/4)\alpha_c}{1+(3/4)\alpha_c} - \Gamma\right)\frac{\gamma_C}{3\alpha_c} \cong 4\pi^2. \tag{35}$$

Since the interior temperature gradient is given by

$$\left.\frac{d\bar{T}}{dz}\right|_{z=0} \cong -\frac{(3/4)\alpha_c}{1+(3/4)\alpha_c},$$

this reduces to the condition $Ra_{RC} = 4\pi^2$ found for the $\kappa = 0$ case. The critical conditions approach each other despite the fact that Θ' as $\kappa \to 0$ does not approach Θ' when $\kappa = 0$ exactly. Whether $\bar{T}$ possesses thin boundary layers or discontinuities near the boundaries does not appear to be as important as the interior value of $d\bar{T}/dz$.

To illustrate the region of validity of these approximations, Fig. 4 depicts the critical Rayleigh number $Ra_C \equiv \gamma_C/\kappa$ versus $1/\kappa$. For small enough κ, the value of Ra_C obtained

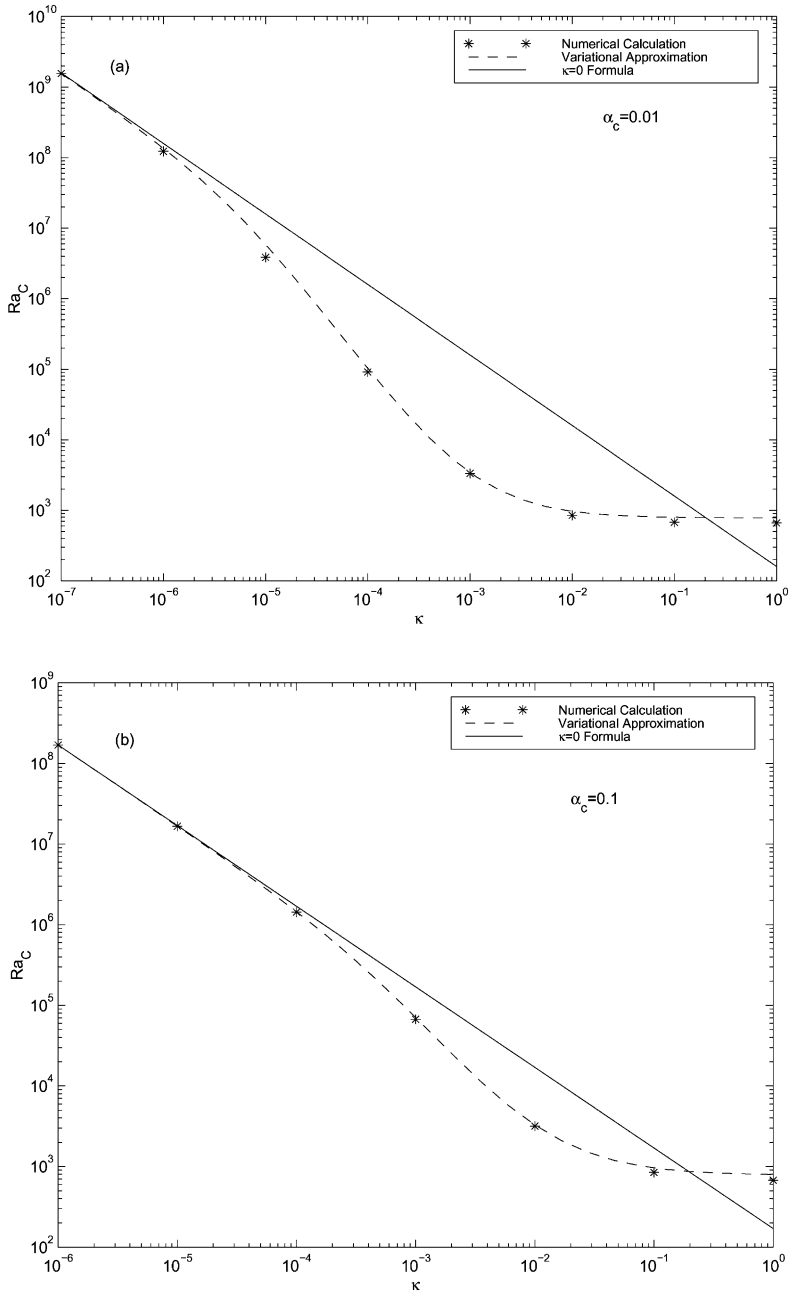

Fig. 4. The critical Rayleigh number $Ra_C \equiv \gamma_C/\kappa$ for linear stability versus the thermal diffusivity κ. The asterisks are obtained from numerical solution of equation (32), the dashed line is obtained from equation (34) with $a^2 = \pi^2$, and the solid line is obtained from equation (28) with $d\bar{T}/dz = -(3/4)\alpha_c/(1 + (3/4)\alpha_c)$. In (a), $\alpha_c = 0.01$; in (b), $\alpha_c = 0.1$ and in (c), $\alpha_c = 1$. In all cases, $\Gamma = 0$. For small enough κ, the solution for $\kappa \neq 0$ approaches the $\kappa = 0$ formula (28).

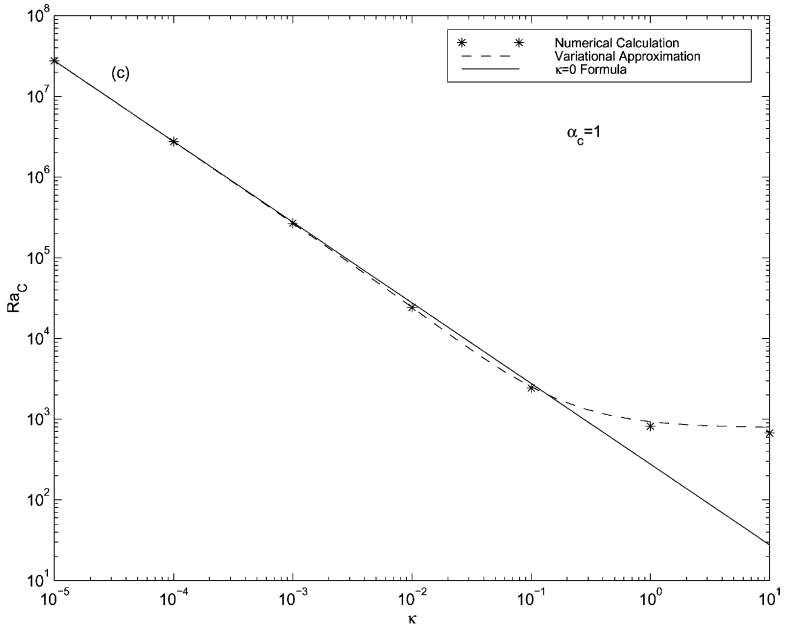

Fig. 4. (*Continued*).

numerically from equation (32) and the estimate of Ra_C obtained from the variational approximation (34) both approach the analytic expression (28) for $\kappa = 0$.

6. Energy stability theory

Linear stability analysis establishes a threshold in *Ra* above which at least one infinitesimal mode grows. In contrast, the energy method establishes a threshold value of *Ra* below which all perturbations, whether infinitesimal or finite-amplitude, decay. The energy stability threshold is always less than or equal to the linear stability threshold. Between the two thresholds lies a region in which subcritical instabilities may or may not exist. To minimize the size of this region of indeterminate stability properties, we strive to bring the energy stability threshold as close as possible to the linear stability threshold. The energy method can yield powerful results because it provides information about nonlinear perturbations.

The energy method involves the construction of an energy equation with generation and dissipation terms. The basic state is stable if the dissipation terms outweigh the generation terms. For the case in which $\kappa = 0$ and $\alpha = \alpha_c$ is constant, the basic state temperature profile is linear, and consequently, we can prove that subcritical instabilities do not exist, as in Rayleigh–Bénard convection (Joseph, 1965). When κ is nonzero, the energy stability threshold lies below the linear stability threshold; in this case, we cannot rule out the possibility of subcritical instabilities.

We now perform an energy stability analysis for our radiative–convective model with arbitrary κ and $\alpha = \alpha_c = \text{constant}$, following the methodology of Straughan (1992). A similar analysis for an idealized atmospheric radiative–convective model has been performed by Larson (2000). The basic state and boundary conditions are the same as for the linear stability problem in Section 5. For later convenience, we introduce the new temperature variable $\hat{T}' \equiv \sqrt{\gamma}\, T'$, but we do not specify the temperature scale $\mathcal{T}_*$ yet. We construct an energy equation as follows. First, we form a kinetic energy equation by dotting $\boldsymbol{v}$ into the momentum equation (5) and averaging over the entire fluid domain. (We assume the perturbations are periodic in the horizontal; then the domain consists of one period cell.) The advection of kinetic energy term vanishes because it represents a redistribution of kinetic energy within the fluid domain rather than a net change. This yields

$$\chi \frac{\mathrm{d}}{\mathrm{d}t}\left\langle \frac{1}{2}\boldsymbol{v}^2 \right\rangle = \sqrt{\gamma}\left\langle w\hat{T}' \right\rangle - \left\langle |\nabla \boldsymbol{v}|^2 \right\rangle, \tag{36}$$

where brackets $\langle\,\cdot\,\rangle$ denote an average over the entire fluid volume. The first term on the right-hand side represents generation of kinetic energy by buoyancy fluctuations, and the second term represents viscous dissipation. Multiplying the heat equation (6) by $\hat{T}'$ and averaging over the entire fluid volume yields

$$\frac{\mathrm{d}}{\mathrm{d}t}\left\langle \frac{1}{2}\hat{T}'^2 \right\rangle = \sqrt{\gamma}\left\langle w\hat{T}'\left(-\frac{\mathrm{d}\bar{T}}{\mathrm{d}z} - \Gamma\right)\right\rangle - \kappa\langle|\nabla\hat{T}'|^2\rangle - \langle 3\alpha\hat{T}'^2\rangle. \tag{37}$$

We have neglected dissipative heating. We now define an "energy" E as

$$E = \chi\langle\tfrac{1}{2}\boldsymbol{v}^2\rangle + \eta\langle\tfrac{1}{2}\hat{T}'^2\rangle,$$

where η is a constant. The energy E is not a real energy, but instead is used as our measure of the perturbation strength. By optimizing the constant η, we may choose this measure so that the energy stability threshold is brought as close as possible to the linear stability threshold.

Combining Eqs. (36) and (37) yields an energy equation

$$\chi\frac{\mathrm{d}E}{\mathrm{d}t} = \sqrt{\gamma}I - \mathcal{D}, \tag{38}$$

where

$$I \equiv \left\langle w\hat{T}'\left(1 - \eta\frac{\mathrm{d}\bar{T}}{\mathrm{d}z} - \eta\Gamma\right)\right\rangle$$

represents generation of E, and

$$\mathcal{D} \equiv \langle|\nabla\boldsymbol{v}|^2\rangle + \kappa\eta\langle|\nabla\hat{T}'|^2\rangle + \eta\langle 3\alpha\hat{T}'^2\rangle$$

represents dissipation. Each term in $\mathcal{D}$ is positive definite. We now define a threshold, γ_E, such that

$$\frac{1}{\sqrt{\gamma_E}} \equiv \max\left(\frac{I}{\mathcal{D}}\right). \tag{39}$$

An upper bound on $\mathrm{d}E/\mathrm{d}t$ is formed by combining Eqs. (38) and (39)

$$\frac{\mathrm{d}E}{\mathrm{d}t} = -\mathcal{D}\sqrt{\gamma}\left(\frac{1}{\sqrt{\gamma}} - \frac{I}{\mathcal{D}}\right) \leq -\mathcal{D}\sqrt{\gamma}\left(\frac{1}{\sqrt{\gamma}} - \frac{1}{\sqrt{\gamma_{\mathrm{E}}}}\right) \equiv -\mathcal{D}A.$$

Suppose now that $\sqrt{\gamma} < \sqrt{\gamma_{\mathrm{E}}}$ so that $A > 0$. Poincaré's inequality (Straughan, 1992) shows that

$$\frac{\mathrm{d}E}{\mathrm{d}t} \leq -\mathcal{D}A \leq -AcE,$$

where c is some positive constant. Integrating in time, we find

$$E(t) \leq \mathrm{e}^{-Act}E(0).$$

Therefore, if $\sqrt{\gamma} < \sqrt{\gamma_{\mathrm{E}}}$, the energy decreases monotonically with time, regardless of the size of the initial perturbation. That is, the basic state is monotonically stable.

To find $\sqrt{\gamma_{\mathrm{E}}}$, we derive and solve the Euler–Lagrange equations for (39) following the standard procedure (Straughan, 1992, pp. 43–44). The Euler–Lagrange equation associated with $\boldsymbol{v}$ is

$$0 = -\nabla\Pi + \frac{1}{2}\sqrt{\gamma_{\mathrm{E}}}\left(1 - \eta\frac{\mathrm{d}\bar{T}}{\mathrm{d}z} - \eta\Gamma\right)\hat{T}'\boldsymbol{k} + \nabla^2\boldsymbol{v}. \tag{40}$$

Here, $\Pi(\boldsymbol{x})$ is a Langrange multiplier which enforces the continuity constraint. Applying $\boldsymbol{k}\cdot\nabla\times\nabla$ to (40) yields

$$0 = \frac{1}{2}\sqrt{\gamma_{\mathrm{E}}}\left(1 - \eta\frac{\mathrm{d}\bar{T}}{\mathrm{d}z} - \eta\Gamma\right)\nabla_{\mathrm{h}}^2\hat{T}' + \nabla^2\nabla^2 w. \tag{41}$$

The Euler–Lagrange equation for T' is

$$-\frac{1}{2}\sqrt{\gamma_{\mathrm{E}}}w\left(1 - \eta\frac{\mathrm{d}\bar{T}}{\mathrm{d}z} - \eta\Gamma\right) = \kappa\eta\nabla^2\hat{T}' - \eta 3\alpha\hat{T}'. \tag{42}$$

We now need to find the smallest eigenvalue $\sqrt{\gamma_{\mathrm{E}}}$ associated with Eqs. (41) and (42). To do so, we substitute in the normal modes equation (16) with wavenumber a. We then minimize the eigenvalue with respect to a^2, holding η fixed. To enlarge the region of monotonic stability, we may, if we so desire, maximize $\sqrt{\gamma_{\mathrm{E}}}$ with respect to η. Restated mathematically, we perform the optimization

$$\sqrt{\gamma_{\mathrm{EC}}} = \max_{\eta}\left(\min_{a^2}\sqrt{\gamma_{\mathrm{E}}}\right).$$

The operations of minimization with respect to a^2 and maximization with respect to η do not commute in general. Therefore, it is safest to perform the minimization with respect to a^2 first.

When $\kappa = 0$ is constant, the basic state temperature profile $\bar{T}$ is linear, and we can rule out subcritical instabilities. We shall set $\eta = 1$, since this turns out to be the optimum value. We choose the temperature scale such that $\mathcal{T}_*/h_*$ equals the basic state lapse rate minus

the adiabatic lapse rate. Then, $-\mathrm{d}\bar{T}/\mathrm{d}z - \Gamma = 1$. The energy method Euler–Lagrange equations for w (41) and $\hat{T}'$ (42) become, respectively,

$$0 = \sqrt{\gamma_\mathrm{E}}\nabla_\mathrm{h}^2\hat{T}' + \nabla^2\nabla^2 w \tag{43}$$

and

$$-\sqrt{\gamma_\mathrm{E}}w = -3\alpha_\mathrm{c}\hat{T}'. \tag{44}$$

We now note that the linear stability of Eqs. (14) and (13) at marginal stability reduce to the energy method of Eqs. (43) and (44), respectively, if we set $s = 0$, $\kappa = 0$, choose the temperature scaling such that $-\mathrm{d}\bar{T}/\mathrm{d}z - \Gamma = 1$, and change variables from T' to $\hat{T}'$. Since the two sets of stability equations and boundary conditions are identical, $\gamma_\mathrm{E} = \gamma_\mathrm{m}$. This completes the proof that no subcritical instabilities exist.

We now consider the case in which $\kappa \neq 0$. We must return to the full Euler–Lagrange Eqs. (41) and (42). These equations are not identical with the linear stability Eqs. (14) and (13), because the basic state temperature profile $\bar{T}$ is no longer linear. We shall find that $\gamma_\mathrm{E} < \gamma_\mathrm{m}$, and we cannot rule out subcritical instabilities. Eqs. (41) and (42) are solved by separating variables and eliminating the temperature variable

$$\begin{aligned}
&\left((D^2 - a^2) - \frac{3\alpha}{\kappa}\right)(D^2 - a^2)^2 W(z) \\
&+\left\{\frac{\eta(\mathrm{d}^3\bar{T}/\mathrm{d}z^3)}{(1-\eta(\mathrm{d}\bar{T}/\mathrm{d}z) - \eta\Gamma)} + \frac{2\eta^2(\mathrm{d}^2\bar{T}/\mathrm{d}z^2)}{(1-\eta(\mathrm{d}\bar{T}/\mathrm{d}z) - \eta\Gamma)^2} + \frac{2\eta(\mathrm{d}^2\bar{T}/\mathrm{d}z^2)}{(1-\eta(\mathrm{d}\bar{T}/\mathrm{d}z) - \eta\Gamma)}D\right\} \\
&\times(D^2 - a^2)^2 W(z) = Ra_\mathrm{E}\left(-\frac{a^2}{4\eta}\right)\left(1 - \eta\frac{\mathrm{d}\bar{T}}{\mathrm{d}z} - \eta\Gamma\right)^2 W(z),
\end{aligned} \tag{45}$$

where the temperature scale is $\mathcal{T}_* = T_{\mathrm{L}_*} - T_{\mathrm{U}_*}$ and $Ra_\mathrm{E} \equiv \gamma_\mathrm{E}/\kappa$. We set $\alpha = \alpha_\mathrm{c}$ and solve this eigenvalue equation for Ra_E numerically. Our computational procedure is to find all eigenvalues and then choose the smallest one. Then, we perform a minimization with respect to a^2 and a maximization with respect to η numerically. The numerical method is described in more detail in Appendix A.

Fig. 5 shows plots of the critical Rayleigh number Ra_EC versus a^2 (circles) from the energy stability problem, superimposed on plots of the critical Rayleigh number Ra_C (asterisks) from the linear stability problem. On these plots, the areas of parameter space below the monotonic stability curves (circles) are stable to arbitrarily large perturbations. The areas above the linear stability curves (asterisks) are unstable to at least one infinitesimal mode. In the areas or gaps between the monotonic and linear stability curves, subcritical instability may or may not occur. In Fig. 5, the largest gap between Ra_EC and Ra_C is about a factor of ten, and it occurs for small optical depth ($\alpha_\mathrm{c} = 0.01$) and small thermal diffusivity ($\kappa = 10^{-7}$). This is probably related to the fact that small α_c and κ imply a highly nonlinear basic state temperature $\bar{T}$. For large κ, the gap between monotonic and linear stability curves is small, which is not surprising since large κ corresponds to the Rayleigh–Bénard limit, for which the monotonic and linear stability curves coincide. Also, as α_c increases, $\bar{T}$ becomes more linear, and the gap between Ra_EC and Ra_C narrows.

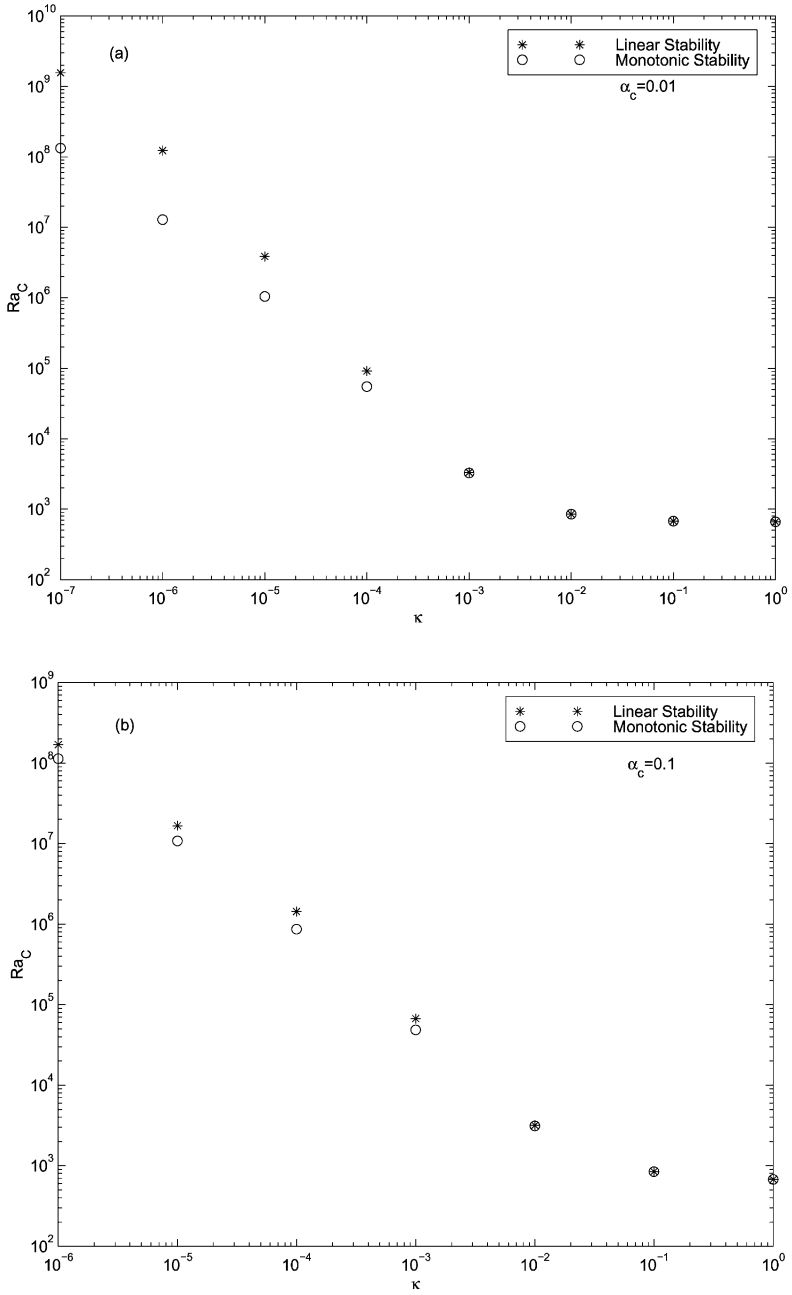

Fig. 5. The critical Rayleigh number Ra_C for linear stability (asterisks) and the marginal Rayleigh number Ra_{EC} for monotonic stability (circles), plotted vs. κ. In (a), $\alpha_c = 0.01$; in (b), $\alpha_c = 0.1$ and in (c), $\alpha_c = 1$. In all cases, $\Gamma = 0$. The region of possible subcritical instability is very small at the larger values of κ and α_c.

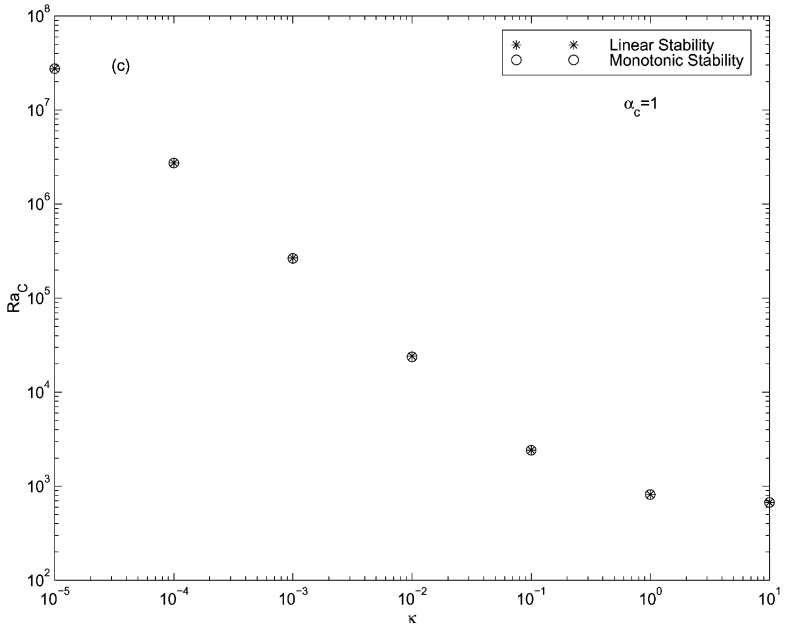

Fig. 5. (*Continued*).

7. Conclusions

This paper has examined Goody's (1956a) radiative–convective model in order to improve physical intuition about the effects of thermal radiation on convection. The main results are summarized below.

First, we examined the linear stability properties when thermal diffusivity κ is set to 0. In this case, the linear stability problem can be solved analytically. Hence, this case serves as a minimal prototype model of radiative–convective instability, just as the Rayleigh–Bénard model serves as a prototype for non-radiative convection. Both linear stability thresholds depend on only a single parameter: for Rayleigh–Bénard convection, this parameter is the Rayleigh number, while for the radiative–convective system, the parameter is a radiative Rayleigh number Ra_{R}. Ra_{R} is defined like the Rayleigh number, but with the interior lapse rate (neglecting temperature jumps at the boundaries) replacing the full lapse rate, and a "radiative diffusivity" replacing the thermal diffusivity. The fact that the stability threshold depends on only one parameter is useful because then the effects of changes in overall temperature and optical depth on stability can be assessed merely by inspection. Increasing the mean temperature T_{m_*} stabilizes the basic state according to the relation $Ra_{\mathrm{R}} \propto T_{\mathrm{m}_*}^{-3}$. When the lapse rate is 0, increasing optical depth α_{c} stabilizes the basic state as $Ra_{\mathrm{R}} \propto 1/(1 + 0.75\alpha_{\mathrm{c}})$. The analytical analysis for the simple $\kappa = 0$ case has relevance to the case when κ is small but nonzero, as in the atmosphere. In particular, the $\kappa \to 0$ linear stability threshold can be characterized approximately in terms of Ra_{R}. However, since $\kappa \to 0$ is a

singular limit, we did find that in this case the perturbation temperature eigenmodes develop thin boundary layers that do not occur in the $\kappa = 0$ case.

Second, we examined nonlinear stability properties. When $\kappa = 0$, we used energy stability theory to rigorously rule out the possibility of subcritical instabilities. For nonzero κ, the behavior is more complicated because the basic state temperature profile $\bar{T}$ is no longer linear. However, energy stability theory yields a threshold below which no infinitesimal or finite-amplitude perturbation may grow. This threshold is useful because it restricts the possibility of subcritical instability to a small range in *Ra* at the larger values of κ and optical depth considered.

A quantitative comparison of our stability thresholds with laboratory experiments is precluded by assumptions such as free-slip boundaries and a radiatively grey gas. One of our qualitative conclusions, however, is a prediction that might be possible to test in a laboratory. Namely, it may be possible to test experimentally whether or not subcritical instabilities exist. Our calculations suggest that subcritical instability can exist only over a small range of *Ra*, particularly at the values of thermal diffusivity ($\kappa \sim 0.1$) appropriate to a laboratory experiment. Bdéoui and Soufiani (1997) have found fair agreement between their detailed linear stability calculations and the laboratory experiment of Gille and Goody (1964). This agreement already hints that for Rayleigh numbers somewhat below the critical Rayleigh number for linear stability, subcritical instabilities do not occur, at least not for initial perturbations as small as experimental noise. (Gille and Goody determined the critical Rayleigh number with an accuracy between 1 and 14%.)

Although this paper has focused on generic features of the interaction of radiation and convection, the absence of strong subcritical instability has specific relevance to the "Ramdas effect" (Ramdas and Atmanathan, 1932). Ramdas noticed that on calm clear nights, air located tens of centimeters above ground sometimes persists at temperatures several degrees cooler than the ground. Such a strong lapse rate is thought to be possible only because of the stabilizing effect of radiative transfer (Vasudeva Murthy et al., 1993; Narasimha and Vasudeva Murthy, 1995). Such layers would be unlikely to persist if they could be easily disrupted by subcritical instability.

Acknowledgements

Kerry A. Emanuel, Richard M. Goody, W.V.R. Malkus, Glenn R. Flierl, R. Alan Plumb, Pablo Zurita, Gerard Roe, and two reviewers read this paper and offered many useful comments. The Department of Energy supported this research via Grant DE-FG02-91ER61220.

Appendix A. Numerical techniques

This appendix describes the numerical methods used to solve the linear and energy stability problems for $\kappa \neq 0$. We follow the textbook of Boyd (1989). The interested reader is directed there for further information.

First, we consider the linear stability problem. Defining the function $V(z)$ by $V(z) \equiv (D^2 - a^2)W(z)$, the linear stability problem (32) can be cast as

$$\left((D^2 - a^2) - \frac{3\alpha_c}{\kappa}\right)(D^2 - a^2)V(z) = Ra\,a^2\left(\frac{d\bar{T}}{dz} + \Gamma\right)(D^2 - a^2)^{-1}V(z) \qquad (A.1)$$

subject to the boundary conditions

$$V|_{z=\pm 1/2} = D^2 V|_{z=\pm 1/2} = 0.$$

This is a generalized eigenvalue problem Press et al. (1992) for the eigenvectors $V(z)$ and eigenvalues Ra. The eigenvalue problem is generalized because operators acting on $V(z)$ appear on both sides of the equation. In our procedure, we choose values of the parameters α_c, κ, Γ, and a^2, compute all eigenvalues Ra and eigenvectors $V(z)$ for these parameter settings, and then select the least eigenvalue and its associated eigenvector.

To resolve the thin boundary layers that appear in the temperature variables $\Theta'(z)$ and $\bar{T}(z)$, fine resolution is needed near the boundaries. For this reason, we use a pseudo-spectral method based on Chebyshev polynomials. That is, we construct a set of basis functions $\{\phi_n\}$, evaluate them on a non-uniformly spaced grid, expand $V(z)$ in terms of the $\{\phi_n\}$ basis, solve for the coefficients of $V(z)$, and finally reconstruct $V(z)$, $W(z)$, and $\Theta'(z)$. Our set of basis functions is denoted

$$\{\phi_n(z)\}, \quad n = 4, 5, \ldots, N+1,$$

where $N+1$ is the highest function represented. We insist that each member of the set $\{\phi_n\}$ satisfy the boundary conditions

$$\phi(z)|_{z=\pm 1/2} = D^2\phi(z)|_{z=\pm 1/2} = 0.$$

To ensure this, we construct each particular basis function ϕ_n by adding to the Chebyshev polynomial T_n, a certain linear combination of the first four Chebyshev polynomials T_0, T_1, T_2, and T_3. Specifically, if we define

$$f(n) \equiv \frac{(n^2-1)n^2}{3} = \left.\frac{d^2 T_n(x)}{dx^2}\right|_{x=1},$$

then for even n,

$$\phi_n(z) = T_n(2z) + (-1 + \tfrac{1}{4}f(n))T_0(2z) - \tfrac{1}{4}f(n)T_2(2z),$$

and for odd n,

$$\phi_n(z) = T_n(2z) + (-1 + \tfrac{1}{24}f(n))T_1(2z) - \tfrac{1}{24}f(n)T_3(2z).$$

Like the higher-order Chebyshev polynomials, each of the functions ϕ_n varies rapidly near its endpoints and relatively slowly in the interior. Therefore, functions possessing boundary layers can be represented accurately with relatively few basis functions. The basis functions ϕ_n are evaluated on an "interior" or "Gauss–Chebyshev" grid which has been modified to span $z = [-1/2, 1/2]$

$$z_j = \frac{1}{2}\cos\left(\frac{\pi(j - 1/2)}{N}\right), \quad j = 1, \ldots, N.$$

The gridpoints are spaced close together near the boundaries and far apart in the interior. Hence, gridpoints are not wasted on the interior region. The functions $V(z)$ and $W(z)$ are expanded in terms of $\phi_n(z_j) \equiv \phi_{jn}$ at the gridpoints z_j

$$V(z_j) = \sum_{n=4}^{N+1} \phi_{jn} \tilde{V}_n, \qquad W(z_j) = \sum_{n=4}^{N+1} \phi_{jn} \tilde{W}_n. \tag{A.2}$$

We want to write the eigenvalue problem in terms of the coefficients $\{\tilde{V}_n\}$. From the definition of $V(z)$, we find that

$$W(z_k) = \phi_{kl} \left(\frac{\mathrm{d}\phi}{\mathrm{d}z} - a^2 \phi \right)^{-1}_{lm} \phi_{mn} \tilde{V}_n. \tag{A.3}$$

Substituting the expressions (A.3) for $W(z_k)$ and (A.2) for $V(z_j)$ into the linear stability equation (A.1), we obtain

$$\sum_{n=4}^{N+1} \left(\frac{-3\alpha_c}{\kappa} + (D^2 - a^2) \right) (D^2 - a^2) \phi_{jn} \tilde{V}_n = Ra \sum_{n=4}^{N+1} a^2 \left(\frac{\mathrm{d}\bar{T}}{\mathrm{d}z} + \Gamma \right)_{jk} \phi_{kl} \left(\frac{\mathrm{d}\phi^2}{\mathrm{d}z^2} - a^2 \phi \right)^{-1}_{lm} \phi_{mn} \tilde{V}_n. \tag{A.4}$$

Here, $(\mathrm{d}\bar{T}/\mathrm{d}z + \Gamma)_{jk}$ is a diagonal matrix with element jj given by $\mathrm{d}\bar{T}(z_j)/\mathrm{d}z + \Gamma$. This eigenvalue problem was solved using the *eig* command from the mathematical software package MATLAB. The *eig* command is based on EISPACK routines. With the spectral coefficients $\tilde{V}_n$ in hand, the spatial functions $V(z_j)$ and $W(z_j)$ can be reconstructed from Eqs. (A.2) and (A.3), respectively. Θ' is obtained from the momentum equation (17). The energy stability eigenvalue problem (45) is solved in a very similar manner.

To find the critical Rayleigh number for linear or monotonic stability, we must minimize with respect to a^2. These minimizations are performed with the golden section search (Press et al., 1992). This method finds local extrema, so we must carefully bracket the desired extremum before commencing the search. The maximization with respect to η in the energy stability problem is optional. In most cases, we use the golden section search to perform the maximization. In some cases in which there is a double minimum with respect to a^2, the golden section search for maximum η fails. We then find an approximate maximum in η by trial and error.

References

Arpaci, V.S., Gözüm, D., 1973. Thermal stability of radiating fluids: the Bénard problem. Phys. Fluids 16, 581–588.

Bdéoui, F., Soufiani, A., 1997. The onset of Rayleigh–Bénard instability in molecular radiating gases. Phys. Fluids A 9, 3858–3872.

Boyd, J.P., 1989. Chebyshev and Fourier Spectral Methods. Springer, New York.

Christophorides, C., Davis, S.H., 1970. Thermal instability with radiative transfer. Phys. Fluids 13, 222–226.

Drazin, P.G., Reid, W.H., 1981. Hydrodynamic Stability. Cambridge University Press, New York.

Getling, A.V., 1980. On the scales of convection flows in a horizontal layer with radiative energy transfer. Atmos. Oceanic Phys. 16, 363–365.

Gille, J., Goody, R.M., 1964. Convection in a radiating gas. J. Fluid Mech. 20, 47–79.

Goody, R.M., 1956a. The influence of radiative transfer on cellular convection. J. Fluid Mech. 1, 424–435.

Goody, R.M., 1956b. Corrigendum. J. Fluid Mech. 1, 670.

Goody, R.M., 1964. Atmospheric Radiation. I. Theoretical Basis. Oxford University Press, New York, pp. 358–360.

Goody, R.M., 1995. Principles of Atmospheric Physics and Chemistry. Oxford University Press, New York.

Goody, R.M., Yung, Y.L., 1989. Atmospheric Radiation: Theoretical Basis, 2nd Edition, Oxford University Press, New York.

Joseph, D.D., 1965. Nonlinear stability of the Boussinesq equations by the method of energy. Arch. Ration. Mech. Anal. 22, 163–184.

Larson, V.E., 2000. Stability properties of and scaling laws for a dry radiative–convective atmosphere. Q. J. R. Meteorol. Soc. 126, 145–171.

Murgai, M.P., Khosla, P.K., 1962. A study of the combined effect of thermal radiative transfer and a magnetic field on the gravitational convection of an ionized fluid. J. Fluid Mech. 14, 433–451.

Narasimha, R., Vasudeva Murthy, A.S., 1995. The energy balance in the Ramdas layer. Bound. Layer Meteorol. 76, 307–321.

Press, W.H., Teukolsky, S.A., Vetterling, W.T., Flannery, B.P., 1992. Numerical Recipes in C: The Art of Scientific Computing, 2nd Edition. Cambridge University Press, New York.

Ramdas, L.A., Atmanathan, S., 1932. The vertical distribution of air temperature near the ground at night. Beit. Geophys. 37, 116–117.

Spiegel, E.A., 1960. The convective instability of a radiating fluid layer. Astrophys. J. 132, 716–728.

Spiegel, E.A., 1962. On the Malkus theory of turbulence. Mécanique de la Turbulence, Center National de la Recherche Scientifique, Paris, pp. 181–201.

Spiegel, E.A., Veronis, G., 1960. On the Boussinesq approximation for a compressible fluid. Astrophys. J. 131, 442–447.

Straughan, B., 1992. The Energy Method, Stability, and Nonlinear Convection. Springer, New York, pp. 43–44.

Vasudeva Murthy, A.S., Srinivasan, J., Narasimha, R., 1993. A theory of the lifted temperature minimum on calm clear nights. Phil. Trans. R. Soc. London A 344, 183–206.

Veronis, G., 1963. Penetrative convection. Astrophys. J. 137, 641–663.

Vincenti, W.G., Traugott, S.C., 1971. The coupling of radiative transfer and gas motion. Annu. Rev. Fluid Mech. 3, 89–116.